Effects of density and velocity changes on the correlation of P-P and P-S reflection events

Alexandru Vant and R. James Brown

ABSTRACT

Assuming that the SEG polarity standard is followed, there will still be cases in which events on the P-P and P-S section have opposite apparent polarities, here called "the unusual situation". This situation makes the correlation and interpretation processes more difficult. To reduce this ambiguity we modelled seismic responses from a wide range of geologically plausible two-layer interface types using acoustic and seismic P- and S-wave velocities and densities measured at confining pressures equivalent to depths up to 2000 m.

The Zoeppritz equations were used to calculate the exact reflection coefficients for a 20° angle of incidence and elastic parameters corresponding to a depth of 1000 m. The results were displayed in plots of R_{PP} versus R_{PS}. In order to investigate the polarity consistency with offset for some of the interfaces mentioned above, we created synthetic velocity and density logs and used them to obtain pseudo-zero-offset gathers together and synthetic stacks.

The unusual polarity situation was found to be associated with geological situations where not all the rock parameters change in the same direction (e.g. velocities increase and density decreases) across the interface. Moreover, in these cases, the changes in elastic parameters are relatively small across the interface and the reflection coefficients are also small when compared to their theoretical range. Although there are exceptions, the polarity generally does not change with offset up to an offset-to-depth ratio of 1.

Later, we exemplify the PP-PS correlation problems that can be created by missing density or shear-wave-sonic logs and also show that the above unusual polarity conditions remain unchanged for interfaces situated at shallower (500 m) and greater (2000 m) depths.

INTRODUCTION

Lately, the interest in multicomponent seismic data and, consequently, for obtaining an improved image of the subsurface has increased dramatically. Therefore, many researchers are making efforts to improve the acquisition, processing and interpretation techniques to better suit the concept of multicomponent seismology (e.g. Lawton et al., 1992; Margrave et al., 2001).

One of the issues that come into play when we try to correlate the P-P and the P-SV seismic sections regards the relative polarities of the matching events from the two sections. In most situations there is a single sign relationship between the two reflection coefficients (R_{PP} and R_{PS}), that is $R_{PP}/R_{PS} < 0$ (Brown et al., 2002). In this 'normal' case the P-P and P-SV events have the same apparent polarity on the records, assuming that recommended polarity standards (Brown et al., 2002) have been observed in the acquisition and preprocessing. Still, there are some reflectors for which the P-P and P-SV

reflections have opposite polarity on the records ($R_{PP}/R_{PS} > 0$). This unusual circumstance can cause problems when we correlate the P-P and P-SV sections.

To reduce the ambiguity in this matter we chose to model as many interface types as possible and compute the P-P and P-SV reflection coefficients for a given angle of incidence. For P-P alone, the best choice might have been normal incidence but, because no converted wave energy is measured at zero offset, a 20° angle of incidence was chosen for all the interface models. For the most interesting interface types, the variation of P-P and P-SV reflection coefficients with offset was also studied. Because most reflection surveys target oil and gas deposits in sedimentary basins, our interest was limited to sedimentary rocks.

THE P-P TO P-SV CORRELATION PROCESS

As a rule the correlation of P-P and P-SV seismic sections is being done through the use of synthetic seismograms. The process is straightforward and requires P-wave sonic, shear-wave sonic and density logs from a well drilled in the vicinity of our multicomponent seismic profile. Synthetic seismograms or synthetic stacks are then created using these logs and events from the sections and synthetics are matched. Finally, events on the P-P stacked section are matched with their counterparts from the P-SV section by using the P-P and P-SV synthetic stacks. The result is usually a stretched P-SV seismic section whose events match their counterparts from the P-P section.

The process is usually complicated by the absence of the shear-wave sonic log and, sometimes, of the density log. When the density log is missing, Gardner's equation (Gardner et al., 1974) is used to calculate density. If the shear-wave or full waveform sonic log is unavailable, then a user-defined V_P/V_S ratio is used to create the P-SV synthetic stack (Lawton et al., 1992). The interval V_P/V_S can then be adjusted to stretch or squeeze the P-SV synthetic stack in a time-variant manner in order to obtain the optimum tie between the synthetic stack and the P-SV stacked section (Miller, 1996). As we will see, the absence of a shear-wave sonic log can lead to synthetic stacks whose polarities are incorrect.

The lack of information about the polarity of the matching events can cause missties of half a cycle between the events on the two sections and, consequently over- or underestimated V_P/V_S ratios for some intervals.

THE POLARITY STANDARD

The polarity standard that is most widely used in industry is the SEG polarity standard for vertical-component geophones and hydrophones (Thigpen et al., 1975). According to Sheriff (2002), this standard says that "the onset of a compression from an explosive source is represented... by a downward deflection..." This implies that, when we use for display the unaltered (minimum-phase) wavelet, a P-wave reflection from an interface with a positive reflection coefficient will begin with a downward deflection on the recorded seismogram (Sheriff, 2002).

In the case of an upgoing converted P-SV wave, the situation is a bit complicated by the fact that for the same event, the signal recorded for negative offsets has reversed

phase compared with that recorded at positive offsets. In this case, the polarity standard is referring to the polarity recorded at positive offsets, the recordings from the negative offsets having their polarities switched in the preprocessing step (Brown et al., 2002).

Although there are no officially adopted SEG standards for P-S data, some recommendations (e.g. Landrum et. al., 1994) state that the onset of an upgoing mode-converted P-SV wave, generated by a compressive source and coming from an interface with a negative reflection coefficient, will be negative on the inline horizontal geophone. Therefore, because for most interfaces, R_{PP} and R_{PS} have opposite signs, the events on P-P and P-SV sections will display the same apparent polarity and will be easily matched. In this chapter, we analyze the situation when events on the two sections display opposite apparent polarities. Throughout the text, we will call this "the unusual situation".

OVERVIEW OF THE DATA USED IN MODELLING

A handful of papers published on AVO and topics related to rock properties (e.g. Castagna et al., 1985; Mavko et al., 1998) analyze the relationships between various elastic or geological rock properties and seismic or acoustic velocities. In this respect, many laboratory measurements have been performed on a wide range of sedimentary rocks. From diverse public data, we selected those containing compressional- and shear-wave velocities and densities for the rocks that are most common to sedimentary basins.

The change of velocity with stress is mainly attributed, for consolidated rocks, to the closure of microcracks, which hardly affects the total porosity but significantly increases the elastic moduli of the rocks. Therefore, we chose to investigate the reflection coefficients for shallow (500 m), intermediate (1000 m) and deep (2000 m) interfaces. Laboratory measurements of acoustic properties of representative rock samples, simulating in-situ effective stress and fluid saturation, proved useful for our modelling.

Although the issue of over- or underpressured formations is very important and is currently considered in many recent research papers (e.g. Prasad, 2002), we chose to leave it aside because it complicates our already unclear polarity problem. In this respect, we only collected velocities that were measured at confining pressures corresponding to the lithostatic pressure at these depths (Figure 1).
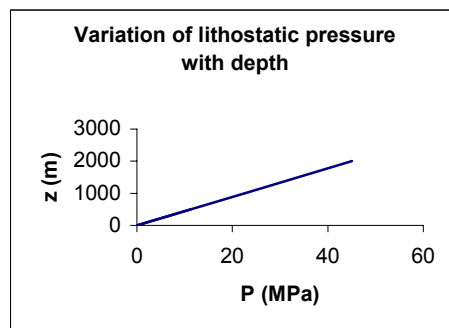
FIG. 1. Variation of lithostatic pressure with depth for an average overburden density of 2.3 g/cm^3.

The corresponding lithostatic pressures were calculated using the formula $P=\rho g z$, where P is the pressure, ρ is the average density of the sedimentary overburden and z is

the depth. We chose $\rho = 2.3$ g/cm^3, which is a reasonable representative value for sediments. The following lithostatic pressure values were obtained: 500 m $\Leftrightarrow$ 11.27 MPa, 1000 m $\Leftrightarrow$ 22.54 MPa, 2000 m $\Leftrightarrow$ 45.08 MPa.

Experimental results show that acoustic velocities in dry and in water- and oil-saturated rock samples usually increase nonlinearly with effective stress over the stress range from 5 to 60 MPa (Bonner and Schock, 1989). Because the published velocities were usually measured at pressures that differ from our calculated values, we assume a linear velocity variation with pressure on the pressure intervals where the velocity measurements are not available (Figure 2) and calculate the velocities at the three specific pressures by means of linear interpolation.
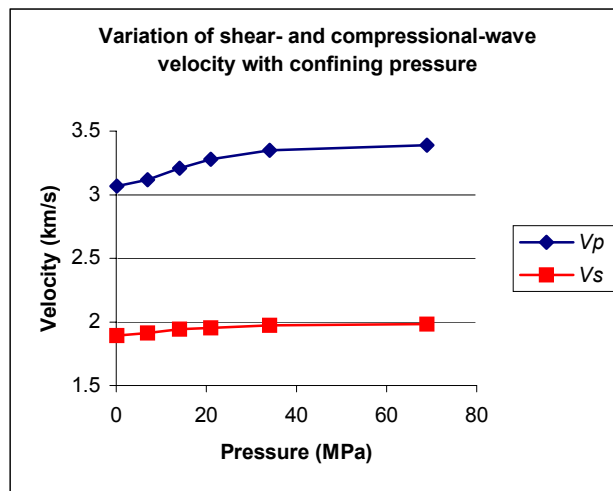
Fig. 2. Variation of shear- and compressional-wave velocity with confining pressure. The example shown is based on data measured on a Boise sandstone sample with ρ =1.93 g/cm^3 (Bonner and Schock, 1989).

MODELLING THE SEDIMENTARY INTERFACES

Choosing the interfaces

Any change in rock property that causes ρ, μ or k to change will, in general, cause seismic velocities to change. For example, going from unsaturated sediment to fluid-saturated sediment will cause both the density and the bulk modulus to change. The bulk modulus changes because air-filled pores become filled with the liquid (water or oil). In this example, the change in shear modulus is insignificant when compared to the change in bulk modulus. Thus, the P-wave velocity changes a lot across the interface while the S-wave velocity changes very little.

There are many different interfaces that could result from the great number of possible combinations of rock types – and also of pore fluids – listed in the table below. As we wanted to investigate in detail only the most plausible such, we had to consider not only the rock types, but also the fluids that saturate their pores.

Eleven satisfactory lithological types were identified. For these rocks, velocity and density measurements have previously been made at a range of confining pressures appropriate to our modelling needs. Then, in accordance with the fluid that saturates each rock type, they were further categorized into nineteen lithotypes. These final lithotypes whose elastic parameters were used for the interface-modelling program are presented in Table 1 together with the type of pore fluid that and their appropriate abbreviations.

Table 1. Rock types used in the interface-modelling program. Classification is based on lithology and pore fluid.

No.	Rock type	Pore fluid	Abbreviation
1	Sandstone	Water	SS-WS
2	Sandstone	Dry/Gas	SS-DR
3	Sandstone	Oil	SS-OS
4	Sand/Poorly consolidated sandstone	Dry/Gas	S-DR
5	Sand/Poorly consolidated sandstone	Water	S-WS
6	Tight gas sandstone	Water	SS-TG-WS
7	Tight gas shale	Water	SH-TG-WS
8	Shale	Water	SH-WS
9	Shale	Dry/Gas	SH-DR
10	Shale	Oil	SH-OS
11	Limestone	Water	LS-WS
12	Limestone	Dry/Gas	LS-DR
13	Dolostone/Dolomite	Oil	DO-OS
14	Dolostone/Dolomite	Water	DO-WS
15	Dolostone/Dolomite	Dry/Gas	DO-DR
16	Coal	Water	CO
17	Salt	-	HA
18	Chalk	Water	CH
19	Gypsum/Anhydrite	-	GY/AN

Possible interfaces

By combining all the 19 rock types obtained above we would have a total of 342 interfaces that are theoretically possible. From the geological point of view though, more than half of them are virtually impossible. Thus, only 124 rock combinations are considered likely to form an interface that would also be geologically valid.

The following reasoning stands behind the choice of interfaces:

Interfaces between two different rock types whose pores are saturated with two different fluids were not considered. In nature, although possible, encountering interfaces where the oil/water, gas/oil or gas/water contact also corresponds to a significant change in lithology is less likely. These types of seismic interfaces where the impedance contrast is produced by change in fluid content are usually encountered inside the same formation (lithostratigraphic unit). Still, we did not consider this second type of interface either.

The decision is motivated by the fact that, although we have velocity and density measurements for the same rock type (e.g., sandstone, limestone, etc.) saturated with different fluids, the measurements were not performed on the same rock samples. For example, the laboratory measurements on water-saturated sandstone were not made on the same rock samples as the measurements made on dry sandstone; that is because provenance of the data is different.

The chance of encountering dry rock in a sedimentary basin is very slim, the majority of sedimentary rocks being water-saturated and in some cases oil- or gas-saturated. So, we decided not to model interfaces with a dry rock component either. Nevertheless, many of the acoustic-velocity measurements were performed on dry rock samples. This is because the physical properties of air are very similar to those of hydrocarbon gas and, of course because it is handier to perform a measurement on a dry than on a gas-saturated sample. Thus, all the measurements made on dry samples were used to model gas-saturated rock.

THE INTERFACE RESPONSE

As shown in the Introduction, the purpose of this research is to model all possible types of sedimentary interfaces and calculate their P-P and P-SV reflection coefficients for an angle of incidence of 20° at depths of 500, 1000 and 2000 m. Although use of the same angle of incidence implies that traces are recorded at different offsets on the P-P and P-SV section, this is not crucial because in the interpretation process we use the final migrated section, on which the spatial location of the P-P and P-S events is the same. Also, the value of 20° for angle of incidence is not particularly significant; it is used to represent a sort of average exploration angle of incidence.

To attain this, we created a computer program, using the MATLAB software. The program uses the *Zoeppritz* function created by Gary Margrave to calculate the exact Zoeppritz P-P and P-SV reflection coefficients for all the possible combinations of interfaces, and then displays the results in R_{PP} versus R_{PS} plots.

To begin with, the results were plotted only for the case when the interface is situated at a depth of 1000 m, which is a typical target depth for many oil and gas deposits. Reflection coefficients obtained for the other two depths (500 and 2000 m) were later analyzed in comparison to those for 1000 m only for the most interesting interface types.

The next step was to eliminate all the unrealistic interface combinations. The results are 124 plots from which this paper only shows a few examples. These plots meet our geological and fluid-saturation-related criteria.

These plots help us to discriminate between the interfaces that would have the same polarity or reversed polarity on P-P and P-S sections. For most of these interfaces, R_{PP} and R_{PS} have opposite signs, but sometimes, they can have the same sign, producing a 180° phase-difference between the events on the P-P and P-S sections plotted using the SEG normal (positive) polarity standard.

The resulting plots can be divided into three basic types (Figure 3):

- Plots in which all points belong to one quadrant (either II or IV).

- Plots in which the points are diagonally spread throughout quadrants II and IV.

- Plots in which the points are diagonally spread throughout quadrants II and/or IV, but in which there are some points that fall into quadrants I and/or III.
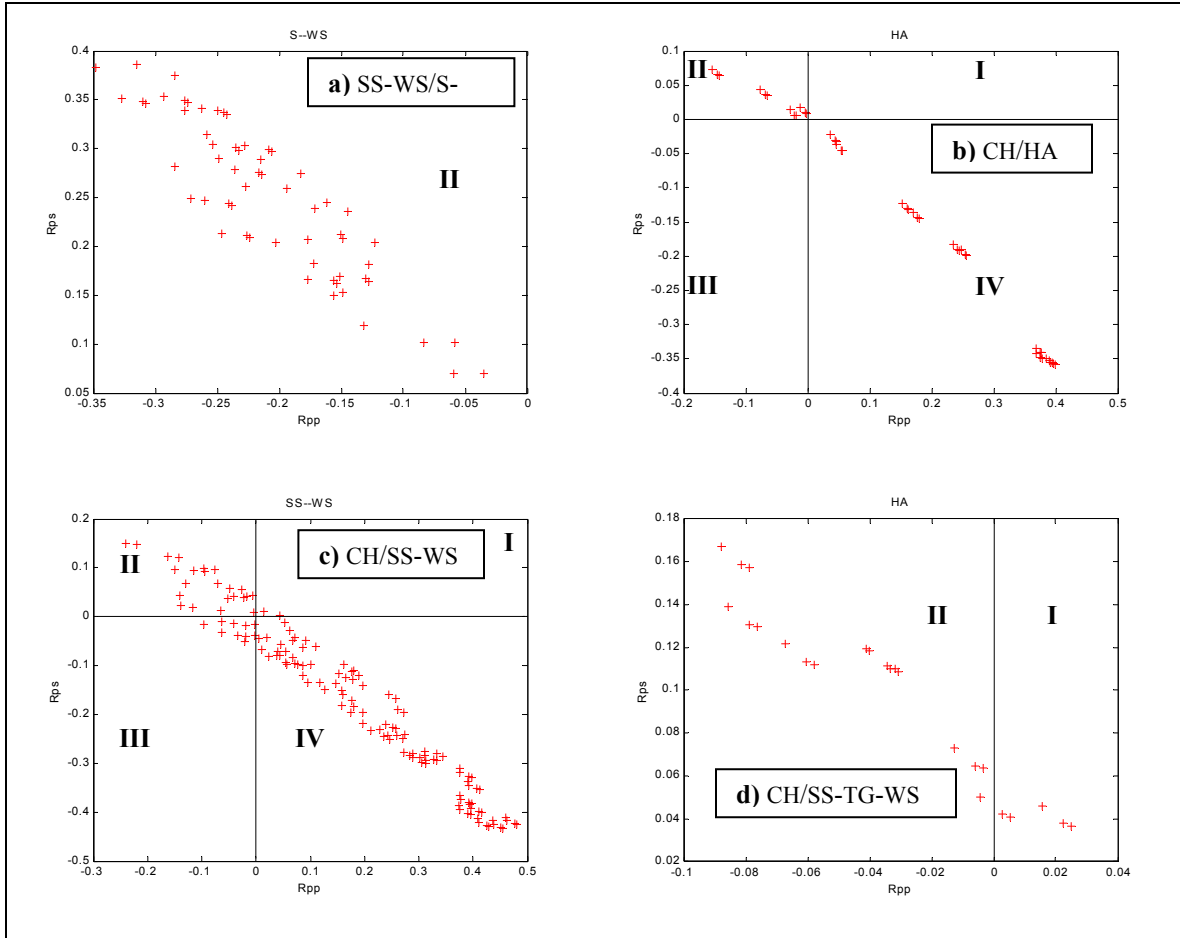
FIG. 3. Examples of R_{PP} versus R_{PS} plots: (a) all points in quadrant II; (b) points in quadrants II and IV; (c) and (d) plots that have some points in quadrants I and/or III.

After plotting results for all the possible interface types situated at the target depth of 1000 m, the next step was to choose from them only the cases where R_{PP} and R_{PS} have matching signs as shown in Figures 3c and d.

From these, we selected for further analysis six interface types that seemed more relevant and for which both P-P and P-SV reflection coefficients have reasonably high values. These interface types are presented in Table 2 and Figures 4 to 6.

Table 2. Interface types that produce a significant number of compressional- and converted-wave reflection coefficients of the same sign.

Interface type		Number of rock samples used in the plot		Figure no.
Overlying rock	**Underlying rock**	**Overlying rock**	**Underlying rock**	
Coal	Chalk	13	10	6
Gas sand	Gas limestone	6	6	5
Gas sandstone	Gas limestone	6	6	5
Water-saturated sandstone	Chalk	10	10	4
Water-saturated sandstone	Water-saturated dolomite	10	5	4
Water-saturated sand	Coal	6	10	6
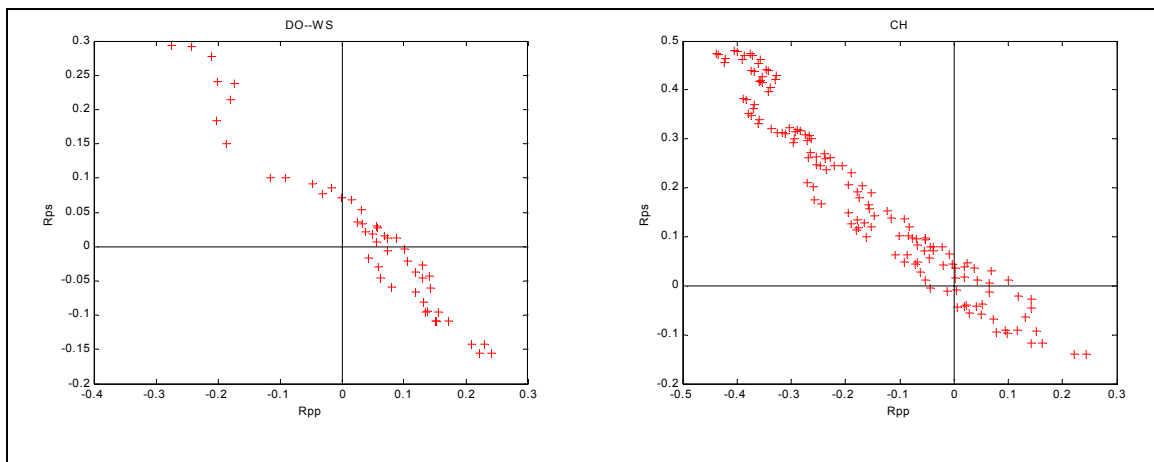
FIG. 4. R_{PP} versus R_{PS} plots for the following interfaces: water-saturated sandstone over water-saturated dolomite (left) and water-saturated sandstone over chalk (right).
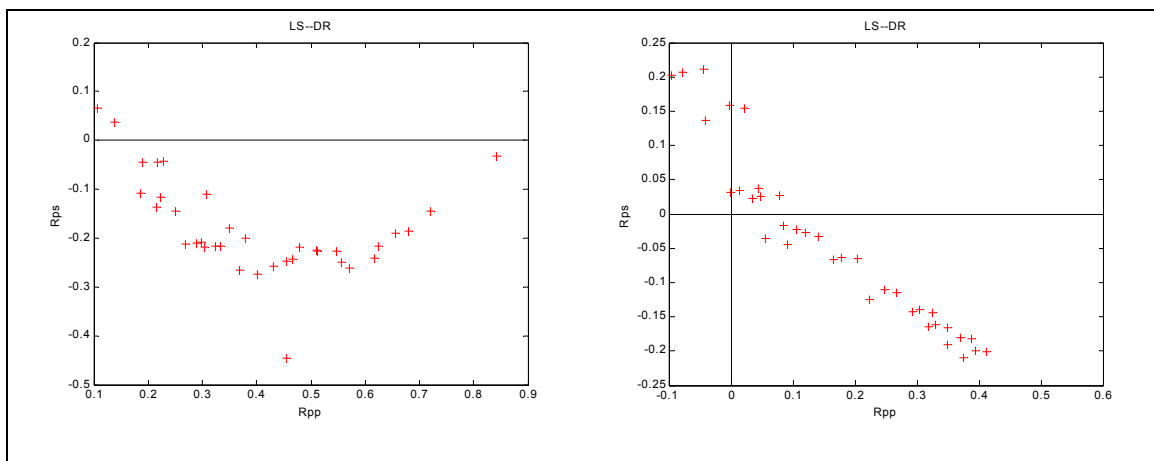
FIG. 5. R_{PP} versus R_{PS} plots for the following interfaces: gas sand over gas limestone (left) and gas sandstone over gas limestone (right).
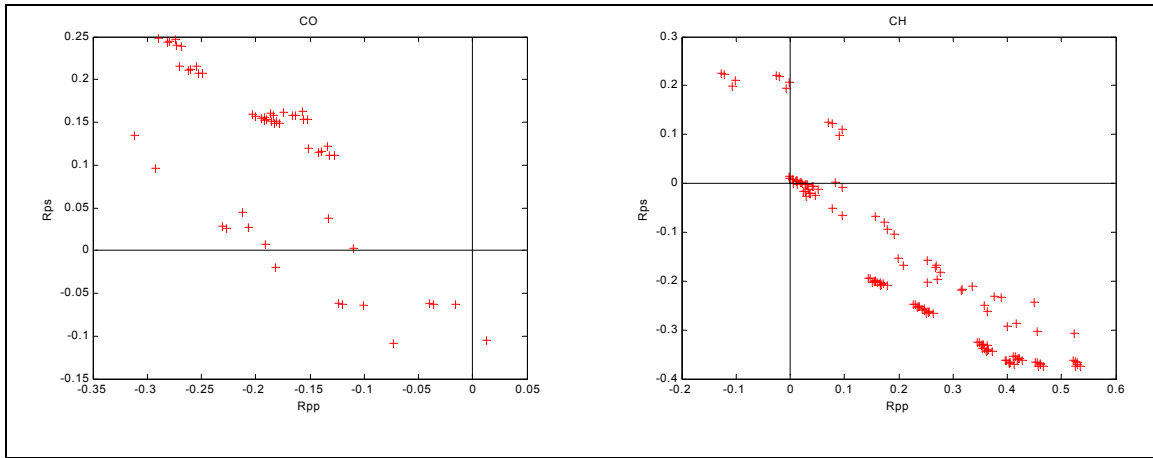
FIG. 6. R_{PP} versus R_{PS} plots for the following interfaces: water-saturated sand over coal (left) and coal over chalk (right).

CREATING SYNTHETIC SEISMOGRAMS

The aim of this study was not only to point out the possible interfaces for which both reflection coefficients have the same sign. We have to keep in mind that, so far, the interface response was investigated only for a 20° angle of incidence. Unfortunately, this is not enough, because the events that appear on a seismic section are the result of common-midpoint stacking in the case of P-P waves and common-conversion-point stacking for P-SV waves.

Because of this, not only do we have to determine the possible interfaces that create the unusual polarity situation, but also to investigate the lateral polarity coherence of the seismic events. For this purpose, we used another MATLAB facility developed by CREWES and called SYNTH. The SYNTH program was originally designed for creating synthetic stacks and, as an input, uses sonic, shear-wave sonic and density logs in LAS format. The synthetic stacks are used for the P-P to P-SV correlation process.

As a first step, for each of the interface types presented in Table 2 and Figures 4 to 6, we pick a representative point from quadrant I or III. We should keep in mind that each point on the R_{PP} versus R_{PS} plots is produced by a unique combination of elastic rock parameters for the interface type considered. For each point chosen from the plot, we extracted the elastic parameters of the two rock samples that create the interface and used them to create synthetic well logs.

These logs were then used as input data for the SYNTH program, the result being pseudo-zero-offset P-P and P-S synthetic seismograms displayed using the normal (positive) polarity and a minimum-phase Ricker wavelet.

The earth response from the chosen interface models

In this section, from the six interface models of Table 3, we present twelve images (Figures 7 and 8) showing the P-P and P-S AVO response and the synthetic stacks. These synthetics were generated from well logs corresponding to the models presented in Figures 4 to 6; all plots are scaled down by the same factor.

For each of the models studied, the P- and S-wave velocities, together with the densities and the corresponding P-P and P-S reflection coefficients, are shown in Table 3. In all the models, the maximum offset-to-depth ratio was set to 1. This ratio covers well the near-offset situation or the short-spread survey.

Table 3. V_P, V_S, ρ and the corresponding P-P and P-S reflection coefficients of the interface models for a 20° angle of incidence.

Interface type	V_P (m/s)	V_S (m/s)	ρ(g/cm³)	R_{PP}	R_{PS}	Fig. no.
Coal	2564	1739	1.37	0.0770	0.1228	7
Chalk	2581.87	1170.36	1.38			
Gas sandstone	3785.67	2591.4	2.0935	0.0420	0.0370	7
Gas limestone	3736.35	2232.54	2.197			
Gas sand	2533.876	1701.43	1.9425	0.1377	0.0370	7
Gas limestone	2816.35	1365.08	2.13			
Water-sat. sandstone	4407.62	2815.08	2.32	0.0030	0.0362	8
Chalk	4080.48	2426.37	2.436			
Water-sat. sandstone	4883.81	3082.54	2.5	0.0554	0.0306	8
Water-sat. dolomite	5168.58	2780.257	2.53			
Water-sat. sand	2398.938	1176.192	1.99918	-0.0730	-0.1087	8
Coal	2702	1851	1.68			

For all but one of the interface models and combinations of elastic parameters shown in Figures 7 and 8, the reflections show phase continuity for both the P-P and P-SV gathers. The exception is the interface model with water-saturated-sandstone over chalk. As offset increases, the P-P gather shows a polarity reversal (Figure 8). Even though the example is singular, it is possible that this type of amplitude variation might be encountered significantly often. In this unfortunate situation, stacking produces a very weak event, which in our case is still showing the same apparent polarity as its P-SV counterpart. This may not have been so, had the polarity reversal appeared on the P-P event at smaller offsets.

This ambiguous situation, associated with a chalk interface, is also encountered in the Alba field from the North Sea, where the top of the chalk formation is produces a strong event on the P-SV section and a very weak one on the P-P section (R. A. Bale, personal communication, 2002).

Next we concentrate on delineating a set of conditions for which the unusual polarity situation appears. The first analysis of the unusual polarity situation that we are aware of was published by Brown et al. (2002). The authors of this paper suggest that this exception is strongly associated with parameter reversals across the interface, meaning that the three rock parameters (the two velocities and the density) do not all change in the same direction across the interface. An example of this occurs when both velocities increase and the density decreases across the interface, etc. In contrast, the normal situation would appear when all three parameters change in the same direction. Indeed, if we analyze the well logs that are plotted in the left part of each synthetic gather, we observe that the same rule applies to our interface examples.
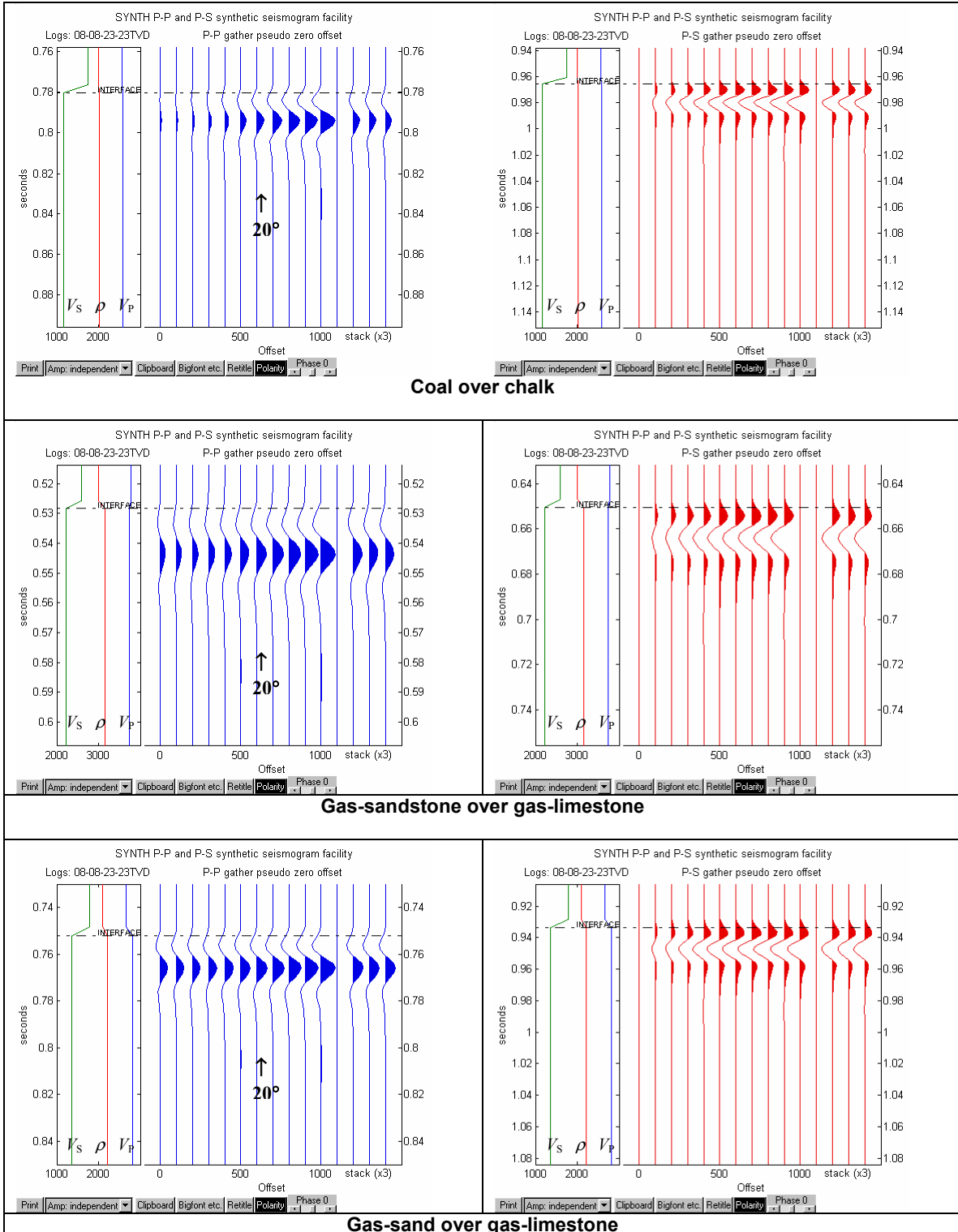
FIG. 7. AVO responses and noise-free synthetic stacks for the first three interface models in Table 3 buried at a depth of 1000 m. The model assumes the upper medium starts from the surface and the lower medium extends down infinitely.
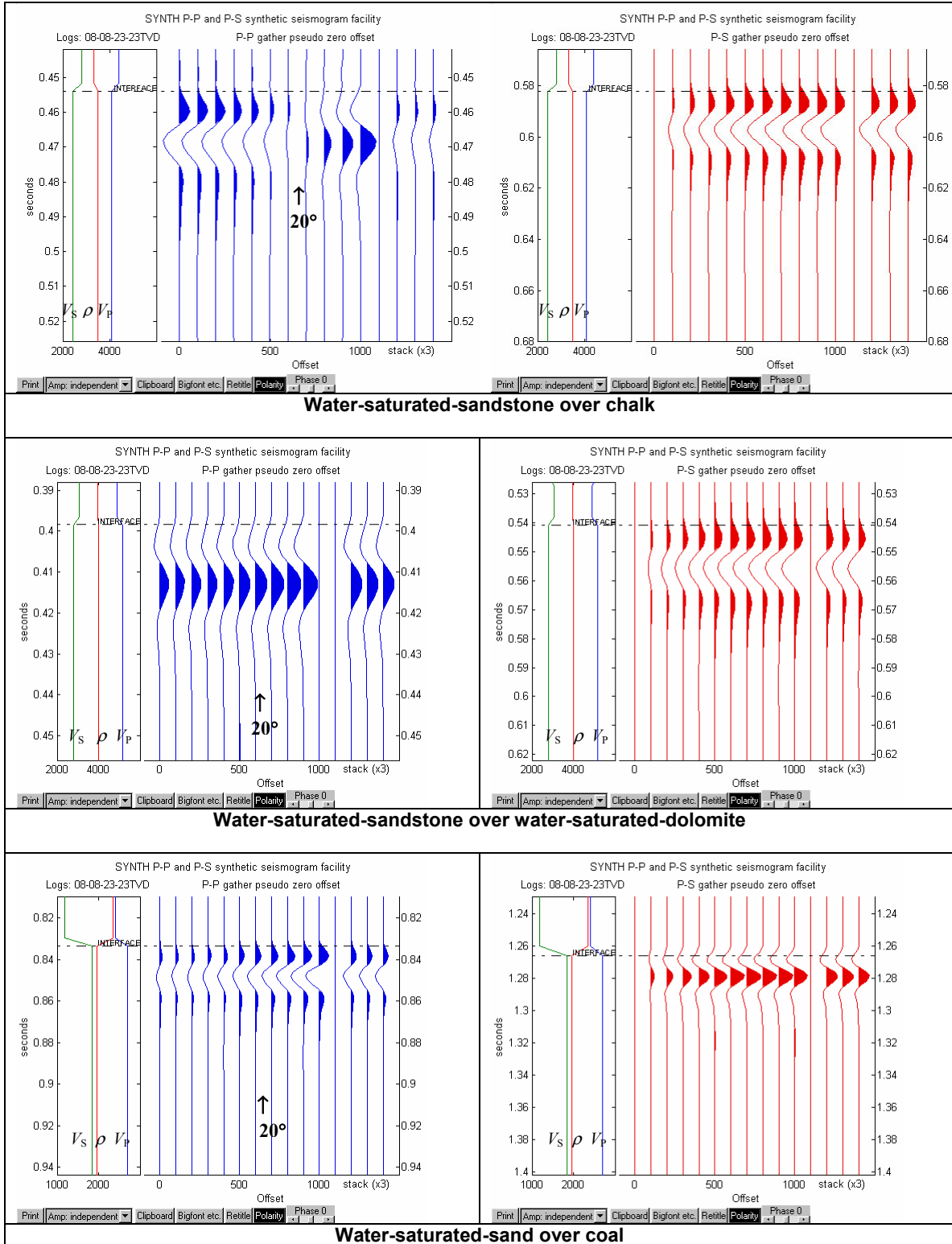
FIG. 8. AVO responses and noise-free synthetic stacks for the last three interface models in Table 3 buried at a depth of 1000 m. The model assumes the upper medium starts from the surface and the lower medium extends down infinitely.

Another pertinent observation is that in all situations, except when we have complex reflection coefficients (e.g. Figure 5, left), if there are points in quadrants III and I they appear in the vicinity of the axis origin and they don't deviate from the general trend of the plot. In all the 124 plots analyzed, both the P-P and P-SV reflection coefficients are fairly small, less than 0.2. As we will show next, the small reflection coefficients are, as expected, associated with certain small changes in rock properties across the interface.

Since the examples shown in this paper cover only a part of the studied pool of situations, we tried to find out if these rules are truly universal. Thus, we picked all the situations where the plots have a significant number of points in quadrants I or III and then ran a statistical analysis of the reflection coefficients and elastic properties.

Table 4 presents a statistical analysis performed on 36 interface types that can produce a significant number of P-P and P-SV reflection coefficients of the same sign.

Variation of the elastic parameters across the interface

As mentioned before, each point in Figures 3 to 6 represents a unique combination of elastic parameters for the two rocks that form the interface. For each interface type, the maximum variation of V_P, V_S and ρ across the interface was calculated. In many of the models, we have velocity changes of up to 100% or more, but only in cases where $R_{PP}/R_{PS} < 0$. In cases where $R_{PP}/R_{PS} > 0$, the parameter variation across the interface is fairly small (Table 4) except for cases with complex R_{PP} values.

- Maximum $|\Delta V_P|$ values range between 6.8 % and 25.8%, with an average of 11.3%

- Maximum $|\Delta V_S|$ values range between 1.5 % and 38.7%, with an average of 18.7%

- Maximum $|\Delta \rho|$ values range between 5.5 % and 31.9%, with an average of 12.4%

The numbers above show that, in the main, the unusual polarity situation coincides with relatively small variations of the elastic parameters across the interface. As a consequence, we can justify using a Shuey-type approximation of the Zoeppritz equations, which assumes small changes in elastic parameters.

For each case when $R_{PP}/R_{PS} > 0$ we also investigated whether the condition of elastic-parameter reversal across the interface is also met (Table 4). They match almost perfectly: with one exception out of 220 cases, each unusual-polarity point on the R_{PP}-versus- R_{PS} figures corresponds to a reversal of the elastic-parameter across the interface.

We also investigated whether the elastic-parameter reversal also appears in cases where $R_{PP}/R_{PS} < 0$. It does. For 35 of 36 interface types (Table 4) there are some situations in which the normal situation is associated with a parameter reversal. Another observation vis-à-vis the trend observed on all the plots is that all the data tend to group diagonally across quadrants II and IV, with some of the points falling into quadrants III and I in the vicinity of the origin.

Table 4. Statistical analysis of the reflection coefficients and the variation of elastic properties across the interface for all interface types that show cases of $R_{PP}/R_{PS} > 0$

Interface	SS-WS				SS-DR		S-DR		S-WS		SS-TG-WS		
	SH-WS	DO-WS	HALITE	CHALK	SH-DR	LS-DR	LS-DR	DO-DR	COAL	CHALK	SH-TG	SH-WS	HALITE
$|\Delta V_P|$ max. (%)	7.8	8.1	12.0	8.8	10.7	13.1	10.0	21.5	16.4	8.6	6.8	9.1	10.2
$|\Delta V_S|$ max. (%)	12.5	17.1	17.6	15.6	19.9	38.7	24.0	37.9	36.5	19.8	10.7	20.7	1.5
$|\Delta\rho|$ max. (%)	9.7	5.5	12.1	6.5	11.7	20.1	8.8	31.9	31.5	6.8	7.1	7.3	10.7
$R_{PP}/R_{PS} > 0$ - point count	3	12	5	12	6	6	2	3	8	10	9	4	5
Parameter-reversal count	3	12	5	12	6	6	2	3	8	10	9	3	5
$R_{PP}/R_{PS} < 0$ - point count	27	38	25	128	18	30	34	45	46	74	31	20	19
Parameter-reversal count	13	17	12	15	15	7	3	9	26	17	14	2	7

Interface	SH-TG	SH-WS			SH-DR		SH-OS	LS-DR				DO-DR	
	SS-TG	SS-WS	SS-TG	DO-WS	SS-DR	LS-DR	HALITE	SS-DR	S-DR	SH-DR	DO-DR	S-DR	LS-DR
$|\Delta V_P|$ max. (%)	6.8	7.8	9.1	11.7	10.7	9.0	16.8	11.6	10.0	9.0	25.9	21.5	65.5
$|\Delta V_S|$ max. (%)	9.9	12.5	20.7	5.0	19.9	14.6	11.7	26.2	24.0	14.6	18.3	37.9	64.9
$|\Delta\rho|$ max. (%)	7.1	9.7	7.3	7.8	11.7	11.4	13.5	20.1	8.8	11.4	25.4	31.9	25.4
$R_{PP}/R_{PS} > 0$ - point count	8	3	5	2	6	2	3	5	2	2	5	4	6
Parameter-reversal count	8	3	5	2	6	2	3	5	2	2	5	4	6
$R_{PP}/R_{PS} < 0$- point count	32	27	19	13	18	22	3	31	34	22	43	44	42
Parameter-reversal count	15	13	0	4	15	6	3	8	3	6	19	8	18

Interface	DO-WS		COAL		HALITE			CHALK		
	SS-WS	SH-WS	S-WS	CH-WS	SS-WS	SS-TG	SH-OS	SS-WS	S-WS	COAL
$|\Delta V_P|$ max. (%)	9.7	11.7	16.4	8.4	12.0	10.2	16.8	8.8	8.6	8.4
$|\Delta V_S|$ max. (%)	17.1	5.0	36.5	32.7	17.6	1.5	11.7	15.6	19.8	32.7
$|\Delta\rho|$ max. (%)	7.0	7.8	20.2	14.3	12.1	10.7	13.5	6.5	6.8	14.3
$R_{PP}/R_{PS} > 0$ - point count	13	2	7	14	3	4	3	12	10	14
Parameter-reversal count	13	2	7	14	3	4	3	12	10	14
$R_{PP}/R_{PS} < 0$- point count	37	13	47	112	27	20	3	128	74	112
Parameter-reversal count	16	4	27	18	14	8	3	15	17	18

If we look now at all data in, say, quadrants II and IV (Figure 3), we observe that R_{PP} is approximately proportional to R_{PS}. That is, an increase or decrease of R_{PP} corresponds to the opposite kind of R_{PS} variation. In contrast, the data in quadrants I and III represent a roughly inverse variation of R_{PP} with R_{PS}.

In conclusion, it can be stated that there is a high probability that sedimentary interfaces across which the elastic parameters change by a small amount, and not all in the same direction, will produce events with opposite apparent polarity on the P-P and P-SV stacked sections.

RELATED INTERPRETATION PROBLEMS

As mentioned in the Introduction, one of the frequent interpretation problems that can be associated with the unusual polarity problem is the matching of events on P-P and P-S sections.

Let's take the case of a seismic reflection acquired using normal (positive) polarity conventions. Provided that one has all the necessary well logs (sonic, shear-wave sonic, and density), the calculated synthetic stacks should display an event having the same polarities as those on the seismic sections (Figure 9 upper part).

The problem arises when shear-wave or full-waveform sonic logs of the survey area are not available. In this case, based on the lithology information available, a constant V_P/V_S ratio is usually chosen. Afterwards, this ratio is modified until the events on the synthetic stack match the events on the section. By assuming a fixed V_P/V_S ratio across an interface, we assume that both velocities vary in the same direction across the interface, which in our example results in the incorrect polarity on the P-SV synthetic stack (Figure 9 lower part). Then, by correlating this biased synthetic stack with the potential seismic section the events are mismatched by half a cycle. Further, it yields an incorrect V_P/V_S ratio; in this case an overestimate.

The same kind of problem can also be triggered by the lack of information on density. Sonic logs are run much more frequently than density logs and in many situations the latter only cover the target zone of the well. Thus, we face the need to generate a synthetic seismogram or stack without density information. Although this is may be a less frequently encountered situation, it is worth studying its effects. When the density log is missing, an empirical formula developed by Gardner et al. (1974) is usually used for determining it. "Gardner's rule" says:

$$\rho = a\alpha^m \tag{1}$$

where α is the P-wave velocity; and the exponent m and the scaling factor a are constants determined by fitting a line to a plot of $\log\rho$ versus $\log\alpha$.

Gardner et al. recommended $m = 0.25$ as being a reasonable value, which was also used in our study. For the factor a, we chose to keep the default value of 310 suggested by the SYNTH package.

As an example, we chose another water-saturated-sand over coal interface. The reason for choosing this interface is that for this rock combination, there is a decrease in both P and S velocities, combined with an increase in density across the interface. The synthetic stacks generated by using all the logs display opposite polarities (Figure 10, upper part), whereas the stacks obtained with Gardner's rule have the same polarity (Figure 10, lower part).
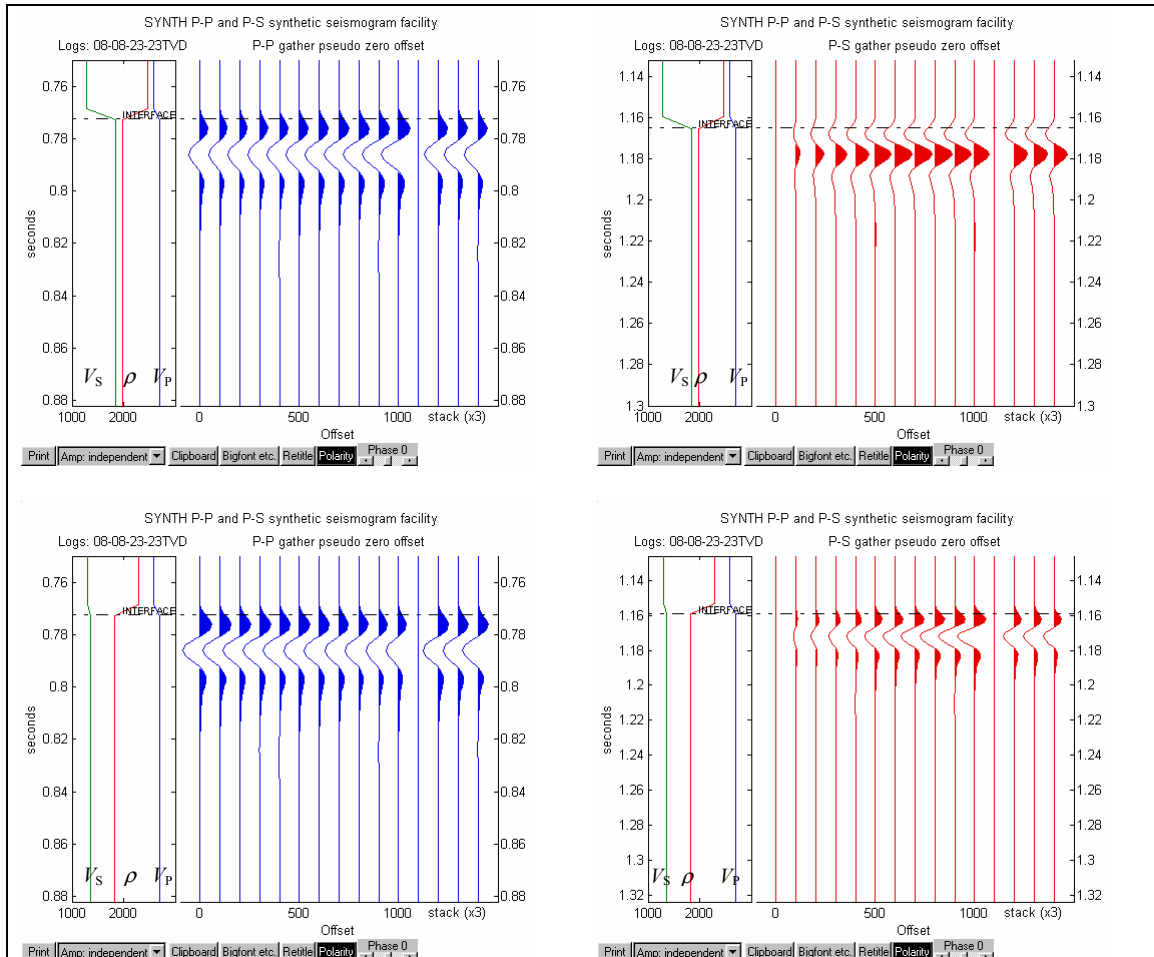
FIG. 9. AVO responses and noise-free synthetic stacks for a water-saturated-sand over coal interface model. All logs were used to create the synthetic stacks (above). The usual V_P/V_S ratio of 2 was used to construct a potentially missing shear-wave sonic log (below)

In this example, the lack of density information affects the P-P synthetic stack, whose polarity is reversed. The reason for this can be seen on the well log plotted in the left part of each stack image. Gardner's rule produces a density log that varies in the same way as the sonic log.

In this section we have shown how the lack of velocity and density information can produce miscorrelations. Errors caused by the lack of shear-wave sonic logs can affect the correlation by leading to the wrong polarity on the P-SV synthetic stack and section. If the density information is not available, the correlation process can be erroneous for particular interface types due to the wrong polarity on the P-P synthetic stack.
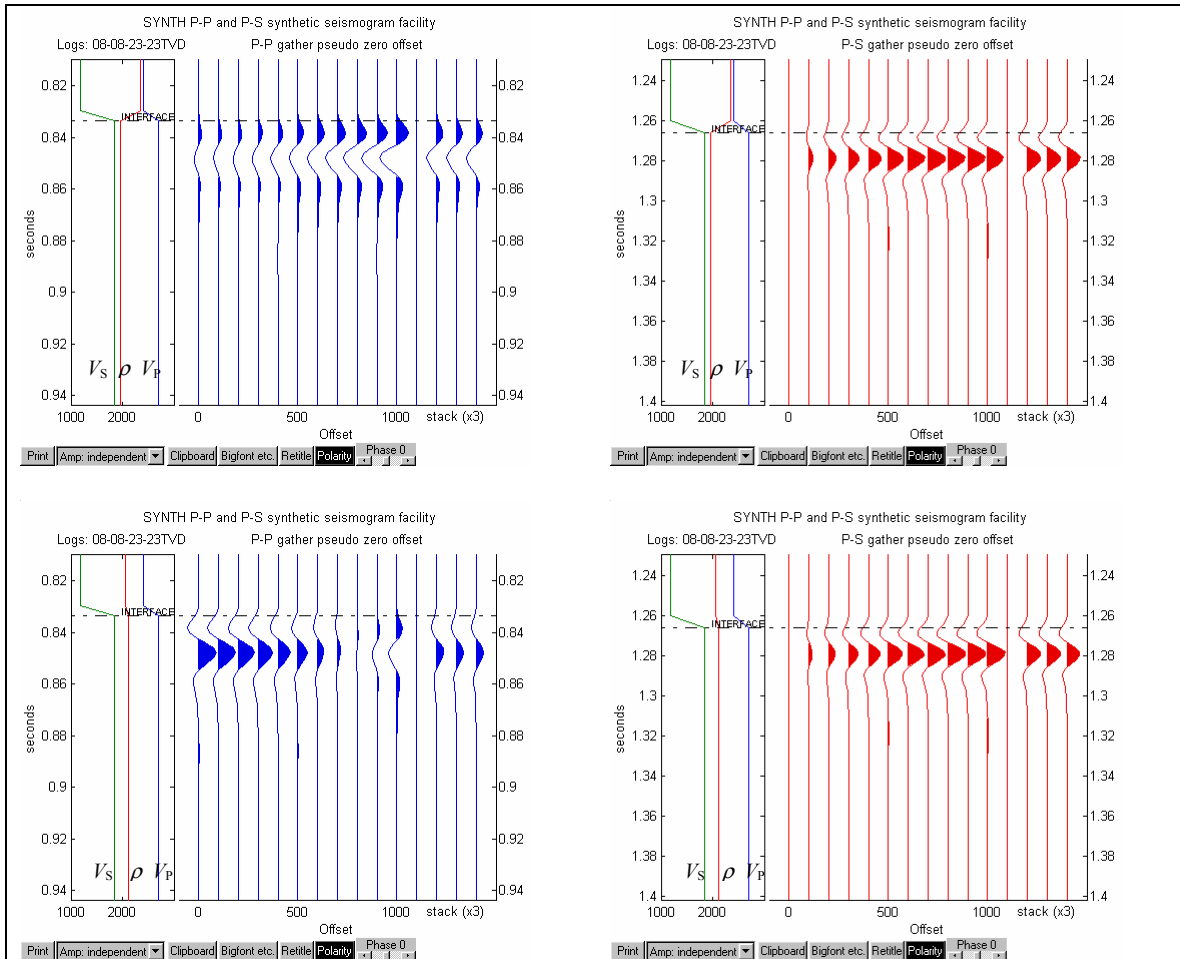
FIG. 10. AVO responses and noise-free synthetic stacks for a water-saturated sand over coal interface model. All logs were used to create the synthetic seismograms (above). Gardner's rule was used for estimating a potentially missing density log (below)

THE VARIATION OF REFLECTION COEFFICIENTS FOR SHALLOW AND DEEP INTERFACES

As mentioned earlier, a criterion used in selecting the input data for the interface-modelling program, was that velocity measurements for a wide range of confining pressures were available. For the completeness of this analysis, we now investigate how the depth of burial affects the distribution of reflection coefficients generated by our interface models.

All the models investigated show a small variation of reflection coefficients with depth, the trend of the plots remaining the same. Although Figure 11 shows just a few examples of water-saturated and gas-saturated interfaces, the observation is also true for all interface types.

The effect of depth on the reflection coefficients is variable, some showing a slight increase and others a slight decrease. The variation is not very significant and we can conclude that the conditions for which $R_{PP}/R_{PS} > 0$ remain substantially the same over the depth range considered in our study.
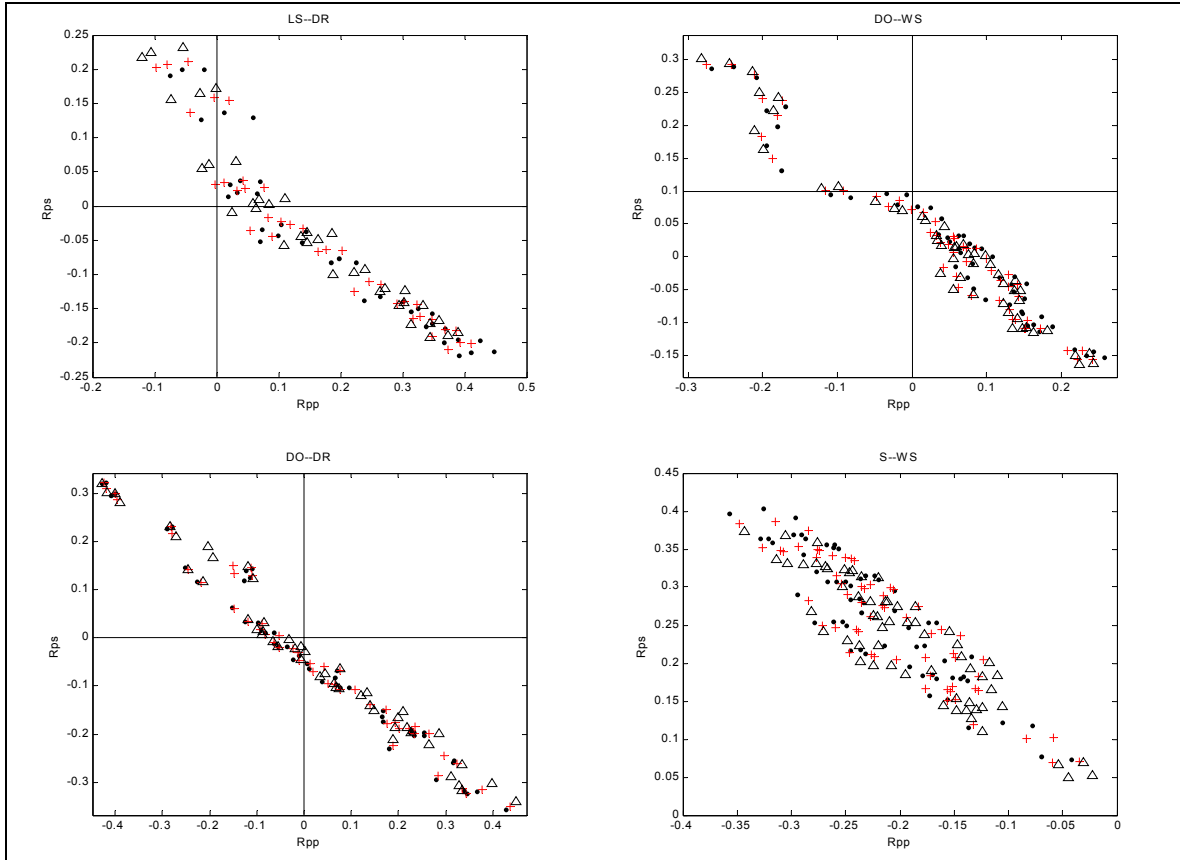
FIG. 11. R_{PP} versus R_{PS} plots for the following interfaces: gas sandstone over gas dolomite (upper left), gas limestone over gas dolomite (lower left), water-saturated sandstone over water-saturated dolomite (upper right) and water-saturated sandstone over water-saturated sand (lower right). Black dots represent a depth of 500 m; red plus signs, a depth of 1000 m; and black triangles, a depth of 2000 m.

CONCLUSIONS

As a result of the interface modelling using real velocity and density data, we can conclude:

- At least for the geological situations covered by our models, the unusual polarity situation was found to be associated with cases in which not all the rock parameters change in the same direction (e.g. P and S velocities change in opposite directions) across the interface.

- In these cases, the changes in elastic parameters are relatively small across the interface and the reflection coefficients are also small when compared to their theoretical range.

- Because changes in parameters are small, the use of a Shuey-type approximation to the Zoeppritz equations can also be used to create the synthetic stacks used in interpretation.

- Although there are exceptions, for most of our models, the pseudo-zero-offset gathers show that apparent event polarity is generally uniform with offset for an offset-to-depth ratio up to 1 at a depth of 1000 m.

- Variation of the elastic parameters with depth does not impact significantly on the reflection coefficients and, although thy show a slight variation with depth, the conditions delineated above remain valid.

REFERENCES

Bonner, B.P. and Schock, R.N., 1989 Seismic wave velocity, *in* Touloukian, Y.S., Judd, W.R. and Roy, R.F., Eds., Physical Properties of Rocks and Minerals: McGraw-Hill Book Co.

Brown, R.J., Stewart, R.R., and Lawton, D.C., 2002, A proposed polarity standard for multicomponent seismic data: Geophysics, **67**, 1028-1037

Castagna, J.P., Batzle, M.L., and Eastwood, R.L., 1985, Relationships between compressional-wave and shear-wave velocities in clastic silicate rocks: Geophysics, **50**, 571-581

Gardner, G.H.F., Gardner, L.W., and Gregory, A.R., 1974, Formation velocity and density: The diagnostic basis of stratigraphic traps: Geophysics, **39**, 770-780

Landrum, R.A., Brook, R.A., and Sallas, J.J., 1994, Polarity convention for vibratory source/recording systems: Geophysics, **59**, 315-322

Lawton, D.C. and Howell, C.E., 1992, P-SV and P-P synthetic stacks: 62nd Ann. Internat. Mtg., Soc. Expl. Geophys., Expanded Abstracts, 1344-1347

Margrave, G.F., Stewart, R.R., and Larsen, J.A., 2001, Joint PP and PS seismic inversion: The Leading Edge, **20**, 1048-1052.

Mavko, G., Mukerji, T., and Dvorkin, J., 1998, The rock physics handbook: Tools for seismic analysis in porous media: Cambridge Univ. Press

Miller, S.L.M., 1996 Multicomponent Seismic Data Interpretation: M.Sc. thesis, Univ. of Calgary.

Prasad M., 2002, Acoustic measurements in unconsolidated sands at low effective pressure and overpressure detection: Geophysics, **67**, 405-412

Sheriff, R.E., 2002, Encyclopedic dictionary of exploration geophysics, 4th ed.: Geophysical References Series, **13**, Soc. Expl. Geophys.

Thigpen, B.B., Dalby, A.E., and Landrum, R., 1975, Special report of the subcommittee on polarity standards: Geophysics, **40**, 694-699.